Toxicology in Vitro 26 (2012) 939–949

Contents lists available at SciVerse ScienceDirect

Toxicology in Vitro

journal homepage: www.elsevier.com/locate/toxinvit

Evaluation of molecularity of rate-limiting step of pore formation by antimicrobial peptides studied using mitochondria as a biosensor

Dinara Aliverdieva [a], Dmitry Mamaev [b,*], Leona Snezhkova [c], Christophor Sholtz [b]

[a] Department of Biotechnology, Caspian Institute of Biological Resources of the Russian Academy of Sciences, ul. Gadjieva 45, Makhachkala 367025, Russia
[b] Laboratory of Biological Oxidation, A.N. Bach Institute of Biochemistry of the Russian Academy of Sciences, Leninsky pr. 33, Moscow 119071, Russia
[c] Educational and Scientific Center, M.M. Shemyakin and Yu.A. Ovchinnikov Institute of Bioorganic Chemistry of the Russian Academy of Sciences, ul. Miklukho-Maklaya 16/10, Moscow 117997, Russia

ARTICLE INFO

Article history:
Received 26 July 2011
Accepted 5 April 2012
Available online 18 April 2012

Keywords:
Alamethicin
Biosensor
Concentration order of reaction
Mastoparan
Melittin
Pore formation mechanism
Potassium transmembrane current
Rat liver mitochondria

ABSTRACT

Toxic agents, derived from bee or hornet venoms and from fungi – melittin, mastoparan, and alamethicin are able to permeabilize biological membranes. We studied the initial steps of pore formation by these peptides in rat liver mitochondria preparations (RLM) generating transmembrane potential ($\Delta\Psi$). RLM has been used as a potassium transmembrane current (PTC) sensor. The PTC induced in RLM depends linearly on the degree of steady-state activation of RLM respiration. The concentration order of such activation by melittin in a "potassium" incubation medium containing 6 mM Mg^{2+} was 2.01 ± 0.15. In the case of mastoparan, the reaction order was 1.83 ± 0.23. The first steady-state phase of activation of RLM respiration by alamethicin was not detected in "Tris" incubation medium; it appeared only after addition of KCl. The order of the reaction limiting such activation was 1.92 ± 0.07. It is suggested that PTC in this phase is determined by the channels with the lowest degree of oligomerization formed by "dimers". The ratio of equally active membrane concentrations of peptides obviously reflects the ratio of average lifetimes (ALT) for corresponding "dimers" (alamethicin and melittin, 38.5; mastoparan and melittin, 0.32). It is concluded that the results of this investigation may be useful for comparative testing of perspective pharmaceuticals.

1. Introduction

There is increasing interest in medical use of toxic pore formers as antimicrobial agents. These include melittin, a 26-residue peptide isolated from *Apis mellifera* bee venom, mastoparans, 14-residue peptide toxins from wasp venoms, and alamethicin, a 19-residue peptide (containing 8 α-aminoisobutyric residues) produced by the fungus *Trichoderma viride* (Duclohier, 2010; Raghuraman and Chattopadhyay, 2007; Yu et al., 2001). Melittin could be an effective agent for preventing liver fibrosis (Park et al., 2011; Lee et al., 2011), inhibition of atherosclerosis (Kim et al., 2011), protection against acute hepatic failure (Park et al., 2012). Melittin restores proteasome function in amyotrophic lateral sclerosis therapy (Jang et al., 2011). Mastoparan and melittin regulate hormone receptor interactions, and therefore these peptides can be used in practical endocrinology (Kamath et al., 2010; Shpakov, 2009). The presence of alamethicin synergistically increased the efficiency of enrofloxacin in treating respiratory diseases caused by *Mycoplasma pulmonis* (Fehri et al., 2007). These studies together focused on the pharmacological effects of low concentrations of low-toxic peptides.

Depending on its oligomerization, alamethicin forms self-organized transmembrane channels of various conductivity and different diameter (Duclohier, 2010). The smallest pores (Hanke and Boheim, 1980) are impermeable for hydrated $Tris^+$ and Ca^{2+} cations, but permeable to K^+. An experimental approach for evaluation of oligomerization of the smallest alamethicin channel did not give clear results (Huang, 2006). In contrast to alamethicin (Sengupta et al., 2008), membrane-bound melittin forms a "pre-pore" existing as a dimer (Takei et al., 1999). It is possible that this stage determines steady-state transmembrane conductivity (Takei et al., 1999). This aggregation of membrane bound mastoparan was demonstrated qualitatively (Schwarz and Reiter, 2001). However, none of these studies reported aggregate structures.

In the membrane-bound state all three of the studied peptides form amphipathic α-helices (Duclohier, 2010; Raghuraman and Chattopadhyay, 2007; Yu et al., 2001). It appears that $\Delta\Psi$ promotes low-energy transformation of the peptide from parallel to perpendicular location relative to the bilayer planar. This precedes channel formation. In the absence of $\Delta\Psi$, almost total transmembrane location of melittin was achieved at the peptide/lipid ratio of 1/10 (Sengupta et al., 2008), whereas in the presence of $\Delta\Psi$ this ratio was close to 1/300 (Kempf et al., 1982). In the case of alamethicin the transmembrane location was achieved at the peptide/lipid ratio of 1/20–1/30 (Shuo Qian et al., 2008) and below

* Corresponding author. Tel.: +7 4959544088; fax: +7 4959542732.
E-mail address: dinara_inbi@mail.ru (D. Mamaev).

0887-2333/$ - see front matter © 2012 Elsevier Ltd. All rights reserved.
http://dx.doi.org/10.1016/j.tiv.2012.04.006

1/100 (Helluin et al., 1997) in the absence and in the presence of $\Delta\Psi$, respectively. In the absence of $\Delta\Psi$, 10% transmembrane location of mastoparan was achieved at the peptide/lipid ratio of 1/10, while in the presence of $\Delta\Psi$ transmembrane location of this peptide was observed at the peptide/lipid ratio of 1/100 (Cabrera et al., 2008).

Most information on pore structure and kinetics of pore formation in liposomes was obtained in the absence of $\Delta\Psi$ and at peptide/lipid ratios of about 1/10–1/40 (Sengupta et al., 2008; Shuo Qian et al., 2008; Cabrera et al., 2008; Pawlak et al., 1991; Matsuzaki et al., 1997; Yu et al., 2001). Under these conditions sigmoidal concentration dependence of activity of antimicrobial peptides is typical. Nonlinear dependence of ratio of parallel and perpendicular peptide location relative to the bilayer planar on total peptide concentration may cause such sigmoidality (Huang, 2006). Total transmembrane location was achieved at the peptide/lipid ratio of 1/10 (Sengupta et al., 2008). The elastic energy of the membrane near a peptide molecule provides an additional driving force for aggregation at ratios of about 1/10–1/20 and thus a simple effect of aggregation can explain pore forming if peptide/lipid ratio has been decreased (Fang-Yu et al., 2002).

Previously, we investigated pore forming effects of 0.02–0.1 μM alamethicin (Sholtz et al., 1985), 0.25–2.4 μM melittin (Sholtz et al., 1980a), and 0.8–4 μM mastoparan (Sholtz et al., 1983) on the rate of succinate oxidation by intact RLM. Under these conditions disturbance of the bilayer in the presence of the peptides is small. In contrast to numerous studies on model membrane systems (Sengupta et al., 2008; Shuo Qian et al., 2008; Cabrera et al., 2008; Pawlak et al., 1991; Matsuzaki et al., 1997; Yu et al., 2001), we always investigated effects of the peptides on intact mitochondrial membrane in the presence of $\Delta\Psi$. The pore forming effects were evaluated by analysis of steady-state rates lasting for several minutes (Sholtz et al., 1985, 1983, 1980a). In calcium-free media in the presence of EDTA and 6 mM magnesium there was suppression of endogenous potassium conductances in RLM (Brierley et al., 1994; Zoratti and Szabo, 1994; Pfeiffer et al., 1995; Belosludtsev et al., 2006; Szewczyk et al., 2009). Such Mg^{2+} concentration has been found in hepatocytes under some physiological conditions (Gaussin et al., 1997; Romani, 2007). In contrast to mitochondria from other tissues, magnesium-independent potassium conductances (Zoratti and Szabo, 1994; O'Rourke, 2007) and UPC (uncoupler protein) channels (Wolkow and Iser, 2006) have not been found in RLM. This suggests that activation of RLM respiration by alamethicin, melittin, and mastoparan in monopotassium media are determined only by transmembrane current through the artificial peptide pores. In the presence of respiratory substrates such cation leakage from RLM is compensated by proton inflow through the proton pump of the electron transport chain and is accompanied by increased mitochondrial respiration (activation of State 4 respiration rate (v_4)) and mitochondrial swelling (Sholtz et al., 1985, 1983, 1980a). RLM are transformed into mitoplasts (i.e. mitochondria with damaged outer membrane but intact inner membrane). Mitoplasts have the same effective system for generation of a proton gradient during succinate oxidation (cf. the H^+/O ratio of 4.6 ± 0.18 and 5.9 ± 0.2 for mitoplasts and RLM, respectively (Hendler and Shrager, 1987). Apparently it is possible to determine the transmembrane current using a biosensor consisting of tightly coupled RLM or mitoplasts and a sensitive oximetric cell. This is a noninvasive and contactless determination that requires only the search for a simple dependence between the transmembrane current and certain properties of RLM ("calibration" of the biosensor).

The aim of this investigation was evaluation of molecularity of rate-limiting step of pore formation by alamethicin, melittin, and mastoparan in the presence of $\Delta\Psi$ at low peptide/lipid ratios using mitochondria as a biosensor; determination of the quantitative relationship between activation of RLM respiration and the cationic current induced in the inner mitochondrial membrane by these antimicrobial peptides. The results of this investigation may be useful for explanation for side effects on mitochondria of low concentrations of these peptides and the mechanism of their hepatotoxicity.

2. Materials and methods

2.1. Materials

The following chemicals were used in this study: protonophores carbonylcyanide(4-trifluoromethoxy)phenylhydrazone (FCCP) (Aldrich)) and 3,5-di-*tert*-butyl-4-oxybenzylidenemalononitrile (SF) (Sumitomo Chem. Co., Japan); rhodamine 123, adenosine-5′diphosphate disodium salt (ADP), valinomycin, 4-(2-hydroxyethyl)-1-piperazineethane sulfonic acid (Hepes) (Sigma, Germany), antimycin A, horse cytochrome *c*, tris(hydroxymethyl)aminomethane (Tris), rotenone, Serva Blue G (Serva, Germany); sucrose (Merck, Germany); alamethicin from *T. viride* (Fluka, Switzerland); KCl, KH_2PO_4 and KOH of specially pure grade, chemically pure succinic acid, $MgCl_2$, ethylenediaminetetraacetic acid (EDTA), ethanol, and dimethylsulfoxide (DMSO) were from Reakhim (Russia) (before use succinic acid and EDTA were recrystallized twice and ethanol and DMSO were redistilled). 2,3-Dihexyl malonic acid was synthesized in our laboratory by D.I. Bondarenko. Mastoparan was isolated from the venom of *Vespa orientalis* as described in (Miroshnikov et al., 1981). Alamethicin synthesized as described in (Rinehart et al., 1977) was a generous gift from Prof. K.L. Rinehart (University of Illinois, USA), and this preparation was used in most experiments. Phospholipase-free melittin was isolated from *A. mellifera* as described in (Gauldie et al., 1976). 1,7,21,23-Tetraacetyl melittin (TAM) was synthesized from melittin as described in (Habermann and Kowallek, 1970). Lack of phospholipase activity was determined as described in (Shipolini et al., 1971).

2.2. Incubation media

Standard incubation medium (SIM) used for determination of the RLM respiratory control (RC) ratio and for study of some effects of mastoparan contained 125 mM sucrose, 2 mM EDTA, 20 mM KCl, 6 mM $MgCl_2$, 10 mM KH_2PO_4, 10 mM sodium succinate, 1.5 μM rotenone, and 20 mM Tris (pH 7.2). We also used monocationic media in which all cations except magnesium were replaced by K^+ or Li^+ and Tris was replaced by Hepes (10 mM), see Table 1.

2.3. Preparation of RLM

Tightly coupled intact RLM were isolated by the modified method of Weinbach using heavy mitochondrial fraction (5500*g*) (Mosolova et al., 1971). In the presence of succinate in SIM the Chance RC value was 5.14 ± 0.65. In $IMKP_{0.3-6}$ and $IMLiP_{0.3-6}$ the RC value was the same. Value v_4 in SIM with succinate as the respiratory substrate was 11.4 ± 0.5 nmol/min/mg RLM protein (data represent mean ± SD for various mitochondrial preparations). In the presence of rotenone, endogenous respiration of RLM represented not more than 6% of v_4. Variations in this parameter did not exceed 4% within each series of respiration curves obtained using one RLM preparation (during 16 h), and within one curve they did not exceed 2–3% during 30 min. In SIM this respiration rate stabilized within 3 min after addition of RLM, and in all other media its stabilization occurred within 5 min. The standard RLM concentration in the oximetric cell was 0.25 mg/ml except for experiments on determination of the partition coefficient (K_p) for distribution of TAM between RLM and the incubation medium.

Table 1
Composition of "monocationic" media.

Medium	Main cation	Buffer	Phosphoric acid	$MgCl_2$	Sucrose	pH
$IMKP_{10-6}$	44 mM K^+	10 mM Hepes	10 mM	6 mM	176 mM	7.5
$IMKP_{1-6}$	35 mM K^+	10 mM Hepes	1 mM	6 mM	194 mM	7.5
$IMKP_{0.3-6}$	35 mM K^+	10 mM Hepes	0.3 mM	6 mM	194 mM	7.5
$IMLP_{0.3-6}$	35 mM Li^+	10 mM Hepes	0.3 mM	6 mM	194 mM	7.5
$IMT_{30}P_{1-6}$	30 mM $Tris^+$	Tris	1 mM	6 mM	209 mM	7.2
$IMT_{70}P_{1-6}$	70 mM $Tris^+$	Tris	1 mM	6 mM	169 mM	7.2
$IMKP_{1-2}$	35 mM K^+	10 mM Hepes	1 mM	2 mM	206 mM	7.5
$IMKP_{0.3-2}$	35 mM K^+	10 mM Hepes	0.3 mM	2 mM	206 mM	7.5
$IMLiP_{0.3-2}$	35 mM Li^+	10 mM Hepes	0.3 mM	2 mM	206 mM	7.5

Note: All "monocationic" media contained 10 mM succinic acid, 2 mM EDTA, 1.5 μM rotenon, 4 μM cytochrome *c*.

2.4. Preparation of submitochondrial particles (SMP)

SMP were obtained by the simplified method of Saint-Macary and Foucher (1985). Briefly, the RLM preparation was placed in hypotonic medium containing 4 mM Tris (pH 7.4) and 2 mM EDTA for 20 min at 0 °C, and after addition of sucrose to 250 mM the mitoplasts were pelleted by centrifugation at 6000*g* for 20 min. The pellet was then suspended in 5 ml of the same medium (with addition of sucrose and 4 μM cytochrome *c*) and sonicated using an MSE ultrasound disintegrator (United Kingdom). The proportion of SMP with intact inner membrane was evaluated after various sonication intervals using 10 μl aliquots.

2.5. Protein determination

RLM protein concentration was determined by a modified method of Bradford (Aliverdieva and Sholtz, 1984) by adding 10 μl of 3% NaOH to 1–5 μl of a concentrated mitochondrial suspension (60–80 mg/ml) and incubating the mixture for 5 min.

2.6. Evaluation of succinate oxidation rate

Rates of succinate oxidation were determined under isothermic conditions (25 °C) with a Clark-type electrode exhibiting a half-time of response of 20 s. The oximeter used in this study reliably assayed respiration rates of 0.2 nmol of O_2/min and the difference in O_2 levels of 2 nM (Aliverdieva et al., 2009).

Oximetric effects of pore formers were normalized by v_4. This minimized errors associated with accuracy of addition of RLM preparations.

Valinomycin, alamethicin, and rotenone (the latter was added just before addition of RLM or SMP to the incubation medium) were added using concentrated stock solutions in ethanol. Rhodamine 123 dissolved in DMSO was added using concentrated stock solution. Melittin, TAM, mastoparan, cytochrome *c*, and KCl were added as concentrated stock solutions in water. Each of the studied effector peptides in their highest concentration activated RLM v_4 to a state stable for 20 min. It appears that the RLM were stable during this time interval.

2.7. Determination of RLM $\Delta\Psi$

RLM $\Delta\Psi$ was determined by changes in fluorescence (F) of rhodamine 123 (excitation at 503 nm and emission at 527 nm) using a Shimadzu RF-5301 PC fluorimeter as described by Emaus et al. (1986). RLM $\Delta\Psi$ was determined in the same media as control oximetric measurements. In separate experiments we demonstrated that a typical pore former causing mitochondrial swelling (alamethicin) did not influence fluorescence during the assay interval (data not shown), and the concentration of the dye did not influence oxidation rates either in the absence or in the presence of any of the peptides used in this study.

2.8. Evaluation of K_p

The value of K_p for the distribution of amphiphilic peptides between respiring RLM and the incubation medium was evaluated according to Sholtz and Zakharova (1980).

2.9. Calculations and data presentation

Data variation is shown for integrated characteristics of the action of the peptide, which were repeated on three different mitochondrial preparations (three independent biological replicates). Plots on figures are representative.

The value of $\Delta\Psi$ was calculated using the empirical equation $-\Delta F/F = (\Delta\Psi - 60)/323$, which describes (for $\Delta\Psi > 66$ mV) a linear part of the corresponding dependence as shown by Emaus et al. (1986). The value of ΔF is the difference between fluorescence values obtained before and after addition of protonophore FCCP or SF. F is fluorescence after addition of FCCP or SF.

The concentration order of the rate-limiting step of pore formation is evaluated as the tangent of the angle between the abscissa and linear dependence of RLM v_4 activation on pore former concentration in double logarithmic coordinates.

Equally active membrane concentration (C_m) corresponding to A_{200} (peptide concentration activating v_4 by 200%) was calculated using the formula $C_m = A_{200} \times 10^{-3}/(1/K_p + \lambda B)$ (Sholtz and Zakharova, 1980), where λ of 0.001 ml/mg is the specific lipid content in mitochondria (it is an estimation of the hydrophobic phase of RLM). B is the concentration of RLM. For $K_p > 1 \times 10^5$, $C_m = A_{200} \cdot 10^{-3}/(\lambda B)$.

3. Results

3.1. Features of mitoplasts from peptide-treated RLM

The use of RLM as a sensor requires demonstration of homogeneity of mitoplasts formed from the peptide-treated organelles. Particularly, it is important to be sure that during the determination procedure the mitoplasts are not enriched in a fraction with damaged inner mitochondrial membrane (which is unable to maintain $\Delta\Psi$). Earlier we demonstrated that in SIM a "succinate oxidase" of RLM is critically (six orders of magnitude) more sensitive to 2,2-dihexyl malonate than succinate dehydrogenase of RLM (Sholtz et al., 1990; Bondarenko et al., 1996). Fig. 1A shows that ultrasonic treatment enriches the mitoplast fraction with inside-out SMP and SMP with damaged inner membrane up to 0.66 evaluated by increased proportion of inhibitor-insensitive "succinate oxidase" $(1-v_2/v_1)$. Fig. 1B shows that treatment of RLM with maximally activating concentration of valinomycin (3 nM) for 14 min was accompanied by insignificant increase in this proportion. Let us assume that the difference in degree of v_4 activation by the SF protonophore and valinomycin is negligible. Such top-heavy

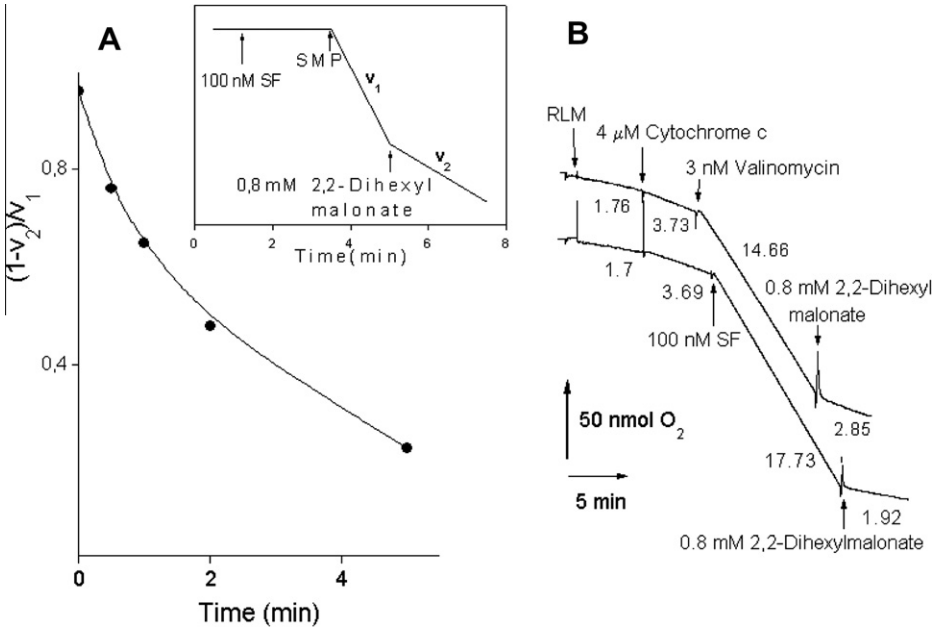

Fig. 1. Effect of 2,2-dihexyl malonate on respiration of RLM subjected to different time course of ultrasonic treatment and activated by SF (A) or activated by SF (upper oxigram) or valinomycin (lower oxigram) without ultrasonic treatment (B). Here and in all other experiments (except data shown in Figs. 8) the concentration of RLM was 0.25 mg/ml. Numbers on oxigrams shows oxidation rates in nmol O_2/min. The inset shows the order of addition of reagents to the medium; v_1 and v_2 are the indications of respiration rates (A). Experiments were performed in SIM medium in the presence of 10 mM sodium succinate and 4 μM cytochrome *c* (A) and also in the absence of cytochrome *c* (B). Plots are representative of three different RLM preparations.

evaluation is used in calculation of the contamination of defective mitoplasts (12.6% excluding antimycin-independent respiration representing 2% of the respiration rate in the presence of the activator). The effect of the studied peptides causing 3- to 4.5-fold activation was measured within 3–6 min, and only treatment with low concentrations causing about 1.5-fold activation was carried out for 14 min. This suggests that the actual contamination by defective mitoplasts during our experiments was significantly lower than that shown in Fig. 1B (and so it was not taken into consideration).

3.2. Effect of valinomycin on RLM v_4

Valinomycin induces PTC in RLM in the presence of $\Delta\Psi$. This inducer is characterized by a rather simple mechanism of action, and its effective concentrations insignificantly disturb membranes. Model experiments demonstrated that PTC could be attributed to electrophoretic movement of equimolar K^+-peptide complexes via the $\Delta\Psi$ gradient, and PTC was proportional to valinomycin concentrations (Naumowicz et al., 2006). Previously we demonstrated (Sholtz et al., 1985) that in SIM containing 6 mM Mg^{2+}, valinomycin activated RLM v_4. Under these conditions endogenous K^+ transporters of RLM were suppressed (details in Section 1). It should be noted that due to a high K_p value for distribution of this peptide between medium and respiring RLM ($(1.8 \pm 0.2) \times 10^5$ (Sholtz et al., 1985), induced PTC was proportional to total concentration of valinomycin in this system. Fig. 2A shows the dependence of the degree of RLM v_4 activation on valinomycin in media containing minimal and maximal K^+ concentrations used in our experiments (20 and 38 mM, curves 2 and 3). In the inset, each point corresponds to v_4 activation after a single addition of peptide. This activation was stable for 16 min. In both media after peptide addition the time of $-\Delta F/F$ stabilization (2 min, Fig. 2B) and the time of stabilization of activation (data not shown) were similar. Linear behavior of the RLM v_4 titration by valinomycin (in one curve) with correlation coefficient more than 0.95 (Fig. 2A) was also preserved in all potassium-containing

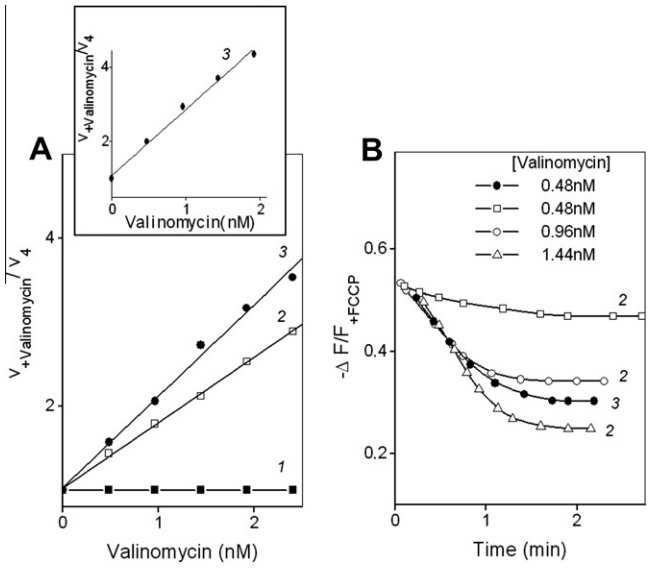

Fig. 2. Dependence of activation of RLM v_4 on valinomycin concentration by titration in one curve (A) and time-dependent changes in relative fluorescence of rhodamine 123 (proportional to $\Delta\Psi$) (B). Designations of media: 1, $IMT_{30}P_{1-6}$; 2, $IMT_{30}P_{1-6}$ + 20 mM KCl; 3, $IMKP_{10-6}$. The inset (A) summarizes results of series of respiration curves obtained using one RLM preparation in $IMKP_{10-6}$, valinomycin was added once in the each curve. For comparison between v_4 activation effect and $\Delta\Psi$, 0.4 μM rhodamine 123 was present for both cases. Other experimental conditions are given in Section 2.7. Plots are representative of three different RLM preparations.

incubation media (SIM, $IMKP_{1-6}$, $IMKP_{0.3-6}$, $IMT_{30}P_{1-6}$ + 20 mM KCl, $IMT_{70}P_{1-6}$ + 20 mM KCl) used in this study (data not shown). Thus, it is reasonable to suggest that in each individual experiment RLM were characterized by a parameter proportional to valinomycin concentration: the degree of activation of v_4 by the peptide. We suggest that PTC is proportional to degree of v_4 activation, and

this proportionality does not depend on the nature of an inducer of the transmembrane current.

3.3. Estimation of concentration order of the PTC-limiting reaction in the presence of melittin

Fig. 3A shows that in $IMKP_{10-6}$ RLM v_4 activation by melittin was stabilized within 5–6 min and synchronously stabilized by $\Delta\Psi$ RLM (Fig. 3B). Here and in subsequent experiments plateaus for all concentrations of the studied peptides were obtained within linearity of corresponding valinomycin "calibration" curves. During measurement of RLM v_4 activation, we added protonophore (FCCP, after valinomycin "calibration" or SF after pore formers). In all these experiments the rate additionally increased from $0.8{\cdot}v_4$ to $3.5{\cdot}v_4$ (data not shown). These results indirectly suggest that the inner mitochondrial membrane maintained its integrity and $\Delta\Psi$.

Tetraacetyl melittin (TAM) showed higher efficiency than melittin, and $\Delta\Psi$ in the region of steady-state v_4 activation (3.5–6 min) decreased monotonously. The value of K_p of TAM between $IMKP_{10-6}$ and respiring RLM (generating $\Delta\Psi$) was according to Sholtz and Zakharova (1980). This K_p value exceeds 10^5 as it does for melittin (Sholtz et al., 1983).

If the v_4 activation degree is proportional to PTC and melittin lacks side effects on the RLM electron transport chain, the concentration order of the limiting reaction (activation) of v_4 induced by this peptide in RLM should be close to two. Since it is limited by dimer pre-pore formation, such value for the order was obtained for the rate of peptide-induced release of a marker dye from liposomes (Takei et al., 1999). Fig. 4 shows the dependence of degree of v_4 activation on melittin concentration in $IMKP_{10-6}$. Under these conditions high value of K_p for melittin between RLM and $IMKP_{10-6}$ (Sholtz et al., 1980a) determines association of the added peptide with RLM, particularly for the inner mitochondrial membrane (as it contains the major proportion of RLM lipids). The concentration order of the studied reaction-limiting activation is 2.16 according to the representative data in the inset of Fig. 4 (2.01 ± 0.15, the mean of three independent determinations). In addition to coincidence of these values under model conditions and in $IMKP_{10-6}$, which was evidence of proportionality of PTC and degree of RLM v_4 activation, in this medium we obtained linear dependence of the activation degree on valinomycin concentration (Fig. 1A). Since this dependence can be obtained rapidly, we applied it as a convenient test for proportionality of such activation and PTC in any medium.

3.4. Rate-limiting step of RLM v_4 activation by melittin and mastoparan

It is known that melittin (Lee et al., 2008), mastoparan (Matsuzaki et al., 1996), and TAM (Stankowski et al., 1991) form large pores in which K^+ and Li^+ mobility is not limited. If pore former-induced conductivity is determined by the rate of cation passage through the pore, the ratio of degree of v_4 activation in $IMKP_{0.3-6}$ and $IMLiP_{0.3-6}$ would be close to the ratio of the transference number for these cations at the concentration of 35 mM at 25 °C, i.e. 1.53 (Ravdel and Ponomareva, 2003). However, according to the representative data of Fig. 5A it is 1.09 (1.12 ± 0.03, the mean of three independent determinations). This independent (but indirect) evidence indicates that pore formation does not limit the melittin-induced transmembrane current in RLM. In liposomes it was shown that melittin-induced permeability was limited by its "pre-pore" formation (Takei et al., 1999). In the case of mastoparan the corresponding ratio was 1.18 ± 0.02 (the mean of three independent determinations, the curves are not shown). In Fig. 6B the corresponding ratio for TAM is 1.4 (1.39 ± 0.01, the mean of three independent determinations). In all cases the corresponding to stabilized RLM v_4 activation $\Delta\Psi$ values for melittin and TAM are basically unchanged in $IMLiP_{0.3-6}$ and $IMKP_{0.3-6}$ (see lower plots in Fig. 5).

3.5. Estimation of concentration order of the PTC-limiting reaction in the presence of mastoparan

In SIM mastoparan stabilized $\Delta\Psi$ synchronously with stabilization of RLM v_4 activation (data not shown). The concentration order of the reaction limiting this activation is 1.76 according to the representative data in the inset of Fig. 6 (1.83 ± 0.23, the mean of three independent determinations).

3.6. Reason for biphasic time dependence curve of RLM v_4 activation in the presence of alamethicin

Previously the first steady-state region on the time-dependent curve of RLM v_4 activation was attributed to PTC through an

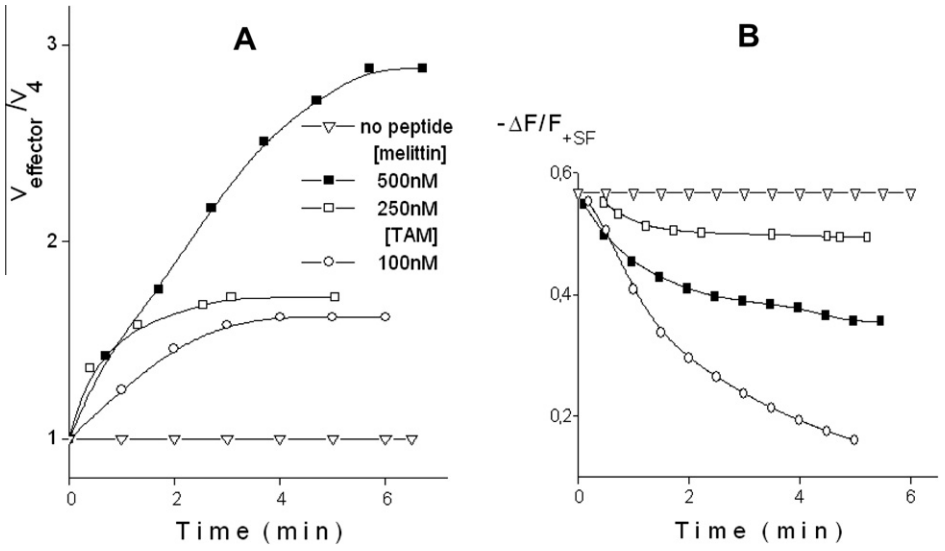

Fig. 3. Time-course of degree of activation of RLM v_4 by 250 and 500 nM melittin in $IMKP_{10-6}$ (A), 100 nM TAM in $IMKP_{1-6}$(B), and time course of changes in relative fluorescence of rhodamine 123 (proportional to $\Delta\Psi$). Plots are representative of three different RLM preparations.

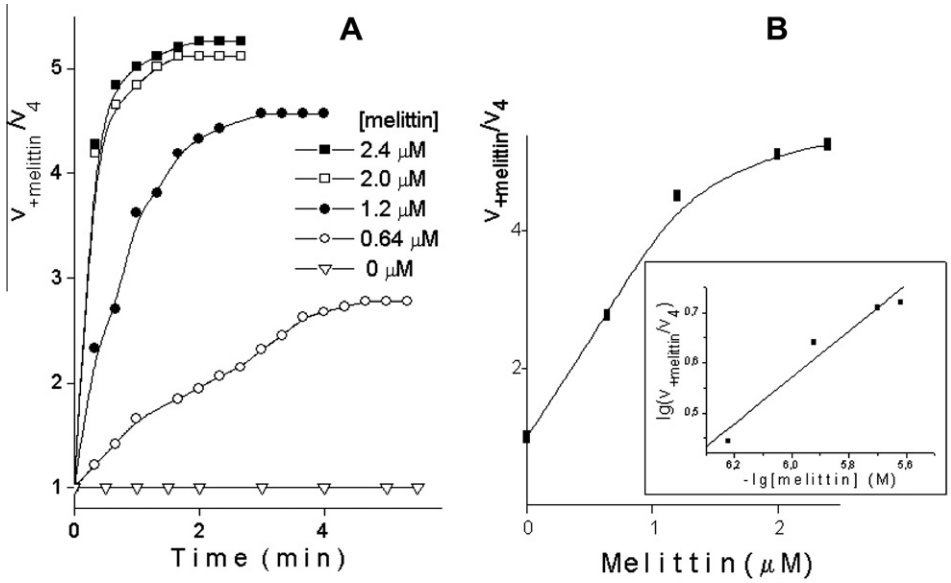

Fig. 4. Time course of degree of activation of RLM v_4 by melittin in $IMKP_{10-6}$ (A) and the dependence of this degree of activation on peptide concentration analyzed on the steady-state region of the time-dependent curves (B); the inset shows data transformation in double logarithmic coordinates. Plots are representative of three different RLM preparations.

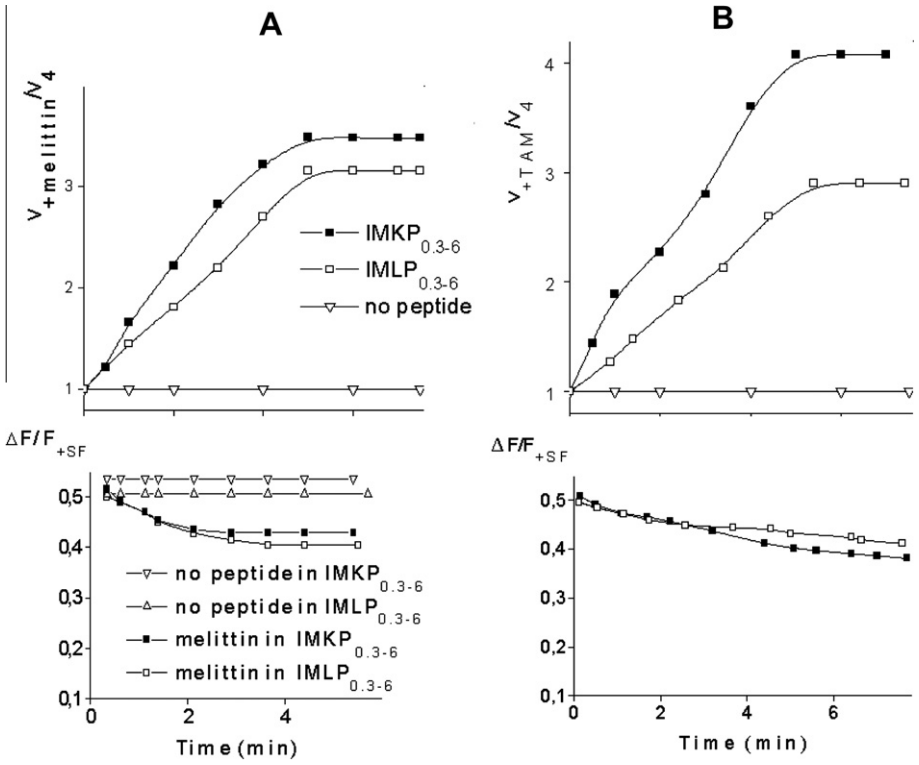

Fig. 5. Time course of degree of activation of RLM v_4 by 0.5 μM melittin (A) and 0.1 μM TAM (B) in the monocationic media $IMKP_{0.3-6}$ and $IMLP_{0.3-6}$ and changes in relative fluorescence of rhodamine 123 (proportional to $\Delta\Psi$). Plots are representative of three different RLM preparations.

alamethicin pore with the lowest oligomerization degree (Sholtz et al., 1985). According to this suggestion, in Fig. 7A the first phase of activation should be absent in the $IMT_{30}P_{1-6}$ medium and appear after addition of K^+. Increasing the $Tris^+$ concentration in media from 30 to 70 mM did not influence the studied dependences (data not shown). In the presence of alamethicin $\Delta\Psi$ synchronous to RLM v_4 activation continuously decreased (Fig. 7B).

3.7. Character of the rate-limiting step in the first phase of RLM v_4 activation by alamethicin

The representative data of Fig. 8A shows that the ratio of degree of steady-state v_4 activation is 1.35 (1.39 ± 0.04, the mean of three independent determinations). This result has to be corrected for the behavior of $\Delta\Psi$ (Fig. 8B) in the region of stabilized RLM v_4

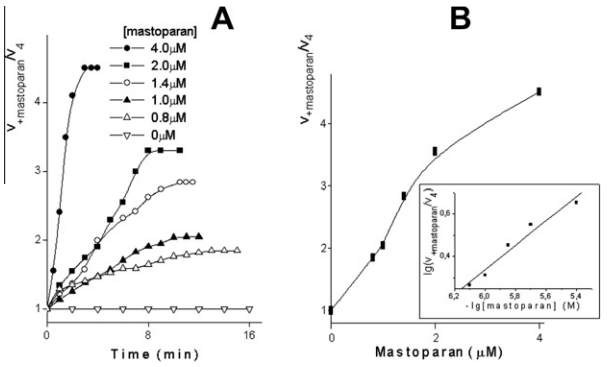

Fig. 6. Time course of degree of activation of RLM v_4 by mastoparan in SIM in the presence of 4 μM cytochrome *c* (a) and the dependence of this degree of activation on peptide concentration analyzed in the steady-state region of the time-dependent curves (B); the inset shows data transformation in double logarithmic coordinates. Plots are representative of three different RLM preparations.

activation. After 0.7 min the $\Delta\Psi$ ratio (calculated using the formula given in Section 2.7.) is 112.3 mV/127.8 mV = 0.879. It is known that ion current in a solution is proportional to potential difference. The decrease in $\Delta\Psi$ in $IMLiP_{0.3-6}$ to the level of the $IMKP_{0.3-6}$ medium yields the true activation ratio of 1.536. After 0.8, 1.0, and 1.15 min the corrected ratios were 1.5, 1.685, and 1.64, respectively. The averaged ratio of activation degrees is 1.59; this value is close to mobility ratios of K^+ and Li^+ in solution (1.53, see Section 3.4.).

3.8. Estimation of concentration order of the first phase of PTC-limiting reaction in the presence of alamethicin

According to model experiments (Hanke and Boheim, 1980) the impermeable for $Tris^+$ and Ca^{2+} alamethicin channels are uniform. Consequently, PTC through these channels is the sum of currents through each single channel. The hydrated diameter of Mg^{2+} is greater than that for Ca^{2+} (Laatikainen et al., 2007), so $IMT_{30}P_{1-6}$, $IMKP_{0.3-6}$, $IMKP_{1-6}$ and $IMLiP_{0.3-6}$ are "quasi-monocationic" media with respect to a low-oligomeric pore.

We investigated the concentration dependence of the first phase of v_4 activation by synthetic alamethicin in the $IMKP_{1-6}$ medium (Fig. 9) and determined the concentration order of the reaction limiting this activation. Earlier we determined the K_p value of $(0.76 \pm 0.01)\cdot 10^3$ for these experimental conditions (Sholtz et al., 1985). This suggests that almost all added alamethicin is in the aqueous phase, and a small quantity of membrane bound peptide (from 5% to 20%) was proportional to its total concentration in the system. Thus, the order determined versus total alamethicin concentration should be close to the order versus its membrane concentration. According to representative data of Fig. 9B it is 1.86 (1.92 ± 0.07, the mean of three independent determinations). Activation of RLM v_4 during formation of a pore, which was not self-organized by sequential addition of monomers as alamethicin, was used as control. The inset of Fig. 7 shows the time-dependent behavior of RLM respiration in $IMT_{30}P_{1-6}$ in the presence of 200 nM TAM. This curve exhibited monophasic behavior.

Side effects of alamethicin on RLM v_4 were evaluated by decreasing Mg^{2+} in the incubation media from 5 to 2 mM. This reduced the concentration order in $IMKP_{1-2}$ to 1.62 ± 0.12 (the mean of three independent determinations). The activation ratio in $IMKP_{0.3-2}$ and $IMLiP_{0.3-2}$ decreased to 1.23 ± 0.05 (the mean of three independent determinations) due to higher activation observed in the $IMLiP_{0.3-2}$ medium (data not shown).

Each RLM preparation in every incubation medium is characterized by the defined slope of valinomycin "calibration" (and apparently the dependence of RLM v_4 activation on PTC). So we estimated the concentration order and the ratio of degree of v_4 activation in $IMKP_{0.3-6}$ and $IMLiP_{0.3-6}$ in the same preparation, but for all constants the variability was calculated using three different preparations.

4. Discussion

Use of RLM as a PTC sensor allowed us to evaluate the molecularity of the rate-limiting step of pore formation by the studied peptides *in situ*. The $\Delta\Psi$ of respiring RLM was stabilized synchronously to the RLM v_4 activation in the presence of melittin or

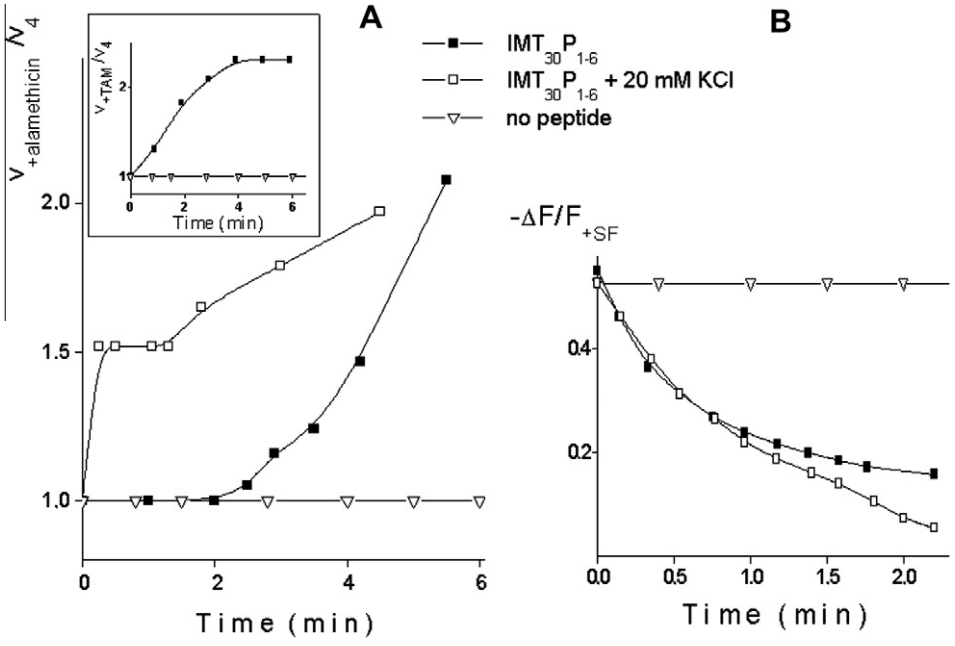

Fig. 7. Time course of degree of activation of RLM v_4 by 110 nM *T. viride* alamethicin in the monocationic medium $IMT_{30}P_{1-6}$ in the presence and in the absence of 20 mM KCl (A) and changes in relative fluorescence of rhodamine 123 (proportional to $\Delta\Psi$) (B). The inset shows the time course of degree of activation of RLM v_4 by 200 nM TAM in the absence of KCl. Plots are representative of three different RLM preparations.

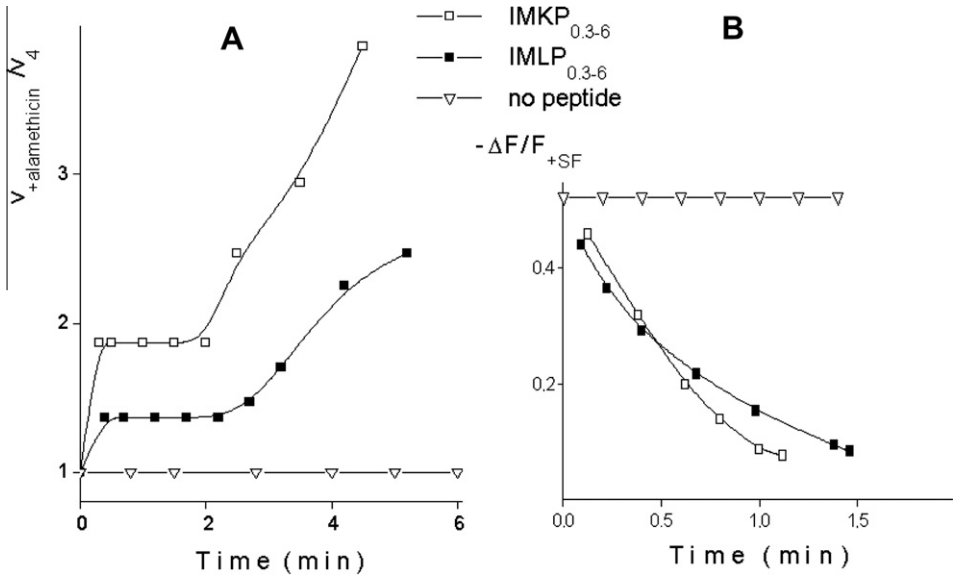

Fig. 8. Time course of degree of activation of RLM v_4 by 110 nM *T. viride* alamethicin in the monocationic media $IMKP_{0.3-6}$ and $IMLP_{0.3-6}$ (A) and changes in relative fluorescence of rhodamine 123 (proportional to $\Delta\Psi$) (B). Plots are representative of three different RLM preparations.

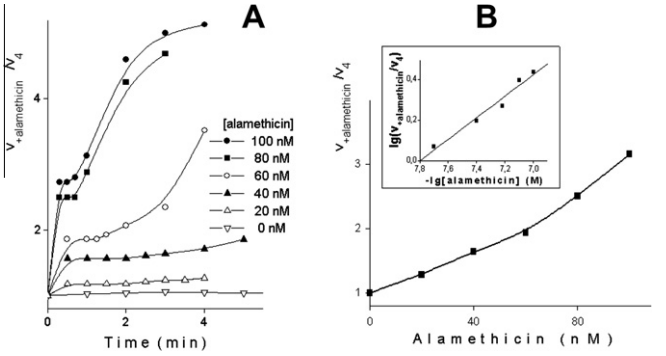

Fig. 9. Time course of degree of activation of RLM v_4 in $IMKP_{1-6}$ by synthetic alamethicin (A) and the dependence of this degree of activation on peptide concentration analyzed in the first steady-state region of the time-dependent curves (B); the inset shows data transformation in double logarithmic coordinates. The concentration of RLM was 0.5 mg/ml. Plots are representative of three different RLM preparations.

mastoparan. Under these conditions peptide molecules attain transmembrane orientation. This activation was limited by association of such monomers to pre-pore. For this association reaction the order values coincided with molecularity or the degree of pre-pore oligomerization, and it was close to two. Using the proposed approach we performed time-dependent separation of steady-state conductivity in the fraction of lowly and highly oligomeric alamethicin channels. The concentration order (and molecularity) of rate limiting reaction of the formation of lowly oligomeric alamethicin channels was close to two. In order to compare parameters of these peptides having the same concentration order of the rate-limiting step of pore formation, we summarized some quantitative parameters described in the Sections 3 (or obtained earlier) in the Table 2.

The Table 2 shows that using our approach it is possible to investigate characteristics of pore formers in the C_m range from 40 to 4600 μM. Taking into consideration average lipid content in RLM (250 nmol/mg RLM protein (Lenton et al., 1995) and specific volume of the lipid phase (10^{-6} ml/mg (Sholtz and Zakharova, 1980), this corresponds to the range of peptide/lipid ratios from 1/6250 to 1/54. At such ratios and in the presence of $\Delta\Psi$ the sigmoidal concentration dependences (Figs. 4B, 5B, 9B) apparently characterize transmembrane peptide monomer association reaction limiting transmembrane current. It should be noted that the molar ratio valinomycin/lipid varied in our experiments (Fig. 2) from 1/625 to 1/125. These ratios are lower than the minimal limit (1/100) determining peptide effect on bilayer structure (Gracheva et al., 1979). If peptide/lipid ratio at critical lytic concentration (CLC) correlates with total bilayer disturbance, at peptide/lipid ratios from 1/6250 to 1/54 we can ignore the cooperativity effect concerned with lipid near peptide molecules. Comparison of lytic and effective peptide concentrations (CLC/A_{200}) suggests that these amphiphiles did not damage the RLM used as the biosensor. Damage did not occur when concentrated peptide preparation is added during 2–3 s into intensively stirred incubation medium with RLM.

Since in the case of the three pore formers channel formation is limited by a bimolecular association reaction ($N = 2$), it is possible to compare the lifetime of the melittin pre-pore and a low-oligomeric pore of alamethicin. In the transmembrane state α-helical monomers of the investigated pore formers are characterized by similar geometrical parameters (Duclohier, 2010; Raghuraman and Chattopadhyay, 2007; Yu et al., 2001). Thus, it is reasonable to suggest similar frequency of their binary collisions in a bilayer. It appears that C_m of alamethicin and melittin reflects average lifetimes (ALT) of a dimer, which depends on the rates of its formation and degradation and also on the rate of its possible conversion into other oligomers. At low concentrations of alamethicin the rate of trimer formation is negligible. Since the rate of transformation of the melittin pre-pore into the pore is lower than the rate of pre-pore formation (Pawlak et al., 1991), the rate of this transformation can also be ignored. For the content of the hydrophobic membrane phase in the formula for C_m we arbitrarily referred to specific lipid content in RLM (λ) (see Section 2.9.). When calculating the C_m ratio for two peptides, the λ parameter is eliminated and we obtained the ALT ratio (38.5) of the melittin pre-pore and a low-oligomeric pore of alamethicin. Analogously, the ALT ratio of the melittin and mastoparan pre-pore is 0.32. Using the proposed approach it is possible to compare ALT for the dimeric state of modified and native pore formers.

Although the toroidal (i.e. lipid-containing) pore model for alamethicin is not popular now (Duclohier, 2010), our results ($N = 2$) do not conflict with the generally accepted viewpoints and

Table 2
Effect of membrane-active peptides on respiring RLM.

Parameter	Peptide (incubation medium)			
	Mastoparan (SIM)	Alamethicin ($IMKP_{1-6}$)	Melittin ($IMKP_{10-6}$)	TAM ($IMKP_{1-6}$)
A_{200}, μM	1.15 ± 0.15	0.065 ± 0.004	0.385 ± 0.015	0.08 (Sholtz et al. (1980a)
K_p	(1.66 ± 0.16) × 10^5 (Sholtz et al. (1983))	(0.76 ± 0.01) × 10^3 (Sholtz et al. (1985))	>>1 × 10^5 (Sholtz et al. (1980a))	>>1 × 10^5
C_m, μM	4600	40	1540	320
CLC, μM	15.6 ± 0.1 (Sholtz et al. (1983))	2.9 ± 0.1 (Sholtz et al. (1985))	3.8 (Sholtz et al. (1980a))	0.6 (Sholtz et al. (1980a))
CLC/A_{200}	13.6	44.6	9.9	7.5
N	1.83 ± 0.23	1.92 ± 0.07	2.01 ± 0.15	–

Notes: A_{200} – peptide concentration activating v_4 by 200%; C_m – equally active membrane concentration corresponding to A_{200} (details in Section 2.9.); CLC – critical lytic concentration (peptide concentration causing lysis of mitochondria); N – concentration order for rate-limiting of RLM v_4 activation by peptide. The values in the table are means of three independent determinations.

experimental data on the interaction of alamethicin with lipid bilayers. This suggests that the alamethicin pore of the smallest diameter contains lipids; this would explain a larger diameter of the channel with lower oligomeric state. Direct analysis of the highly oligomeric structure of alamethicin pores (Shuo Qian et al., 2008) visualized its protein-like nature, which was described by the barrel-stave model (Duclohier, 2010). Our results correspond to the literature data on the concentration order reaction value of four determined for the alamethicin pore permeable for the large Pr^{3+} ion in liposomes (Hunt and Jones, 1982). In the protein-like pore model the inner diameter of the channel with oligomerization degree of five corresponds to hydrated K^+ (Duclohier, 2010). A transmembrane peptide monomer forms a hole in both lipid monolayers; collision of monomers (or even close positioning) produces thinning of the membrane around the helical bundle. This promotes electroporation, formation of a lipid–peptide pore and, possibly, its stabilization (i.e. increase in its ALT compared with a purely lipid pore) (Kessel et al., 2004). The toroidal pore formed by alamethicin facilitates transfer of the peptide from the outer to the inner membrane monolayer with monomer reversal (as described for magainin (Huang, 2006)). Additional stabilization of the pore might by achieved due to energetically favorable (“head to tail”) association of two transmembrane monomers (Mottamal and Lazaridis, 2006). The effect of lipid properties on channels with various oligomerization degrees was investigated using bilayer lipid membranes (BLM). The ALT of the lowest conductance state of the alamethicin pore was more sensitive to pH-dependent variation of the membrane surface potential and modulators of membrane dipole potential (Mereuta et al., 2011). The aggregation variant of the barrel-stave model is applied to lowly and highly oligomeric pores (Duclohier, 2010). The ALT channel sensitivity should be the same because pores undergo self-conversion using the same reaction of association or dissociation of a monomer. Thus, we suggest the toroidal pore model for the lowly oligomeric channel of alamethicin and cannot exclude a purely peptide pore formed by highly oligomeric alamethicin.

Let us compare advantages and limits of the RLM-based biosensor with traditional methods used for studies of pore formers. Using RLM preparations it is possible to measure a value ($v_{+peptide}/v_4$) that is proportional to cationic current induced by valinomycin, melittin, and mastoparan (Figs. 2A, 3A, 5A) at stabilized $\Delta\Psi$ (Figs. 2B, 3B). Maintenance of constant $\Delta\Psi$ across a liposomal membrane requires use of additional complex procedures. For example, a concentration gradient of potassium ions inside and outside large liposomes with isoosmotic compensation maintains constant $\Delta\Psi$ only during the initial moments of the permeability assay (Polozov et al., 1997). In RLM the functionally competent respiratory chain generates $\Delta\Psi$ for several minutes (Figs. 2B, 3B, 6, 7B, 8B), so during determinations of concentration order of peptide association reactions all peptide molecules are in transmembrane position. Determination of concentration dependence of steady-state RLM v_4 activation (reflecting PTC) requires fewer experiments than determination of initial rates of pore former-induced leakage of a marker dye from liposomes. Use of the “all-or-none leakage” model describing melittin-induced release of a marker dye (Schwarz and Reiter, 2001) is not applicable for mastoparan (Cabrera et al., 2008).

Using the RLM biosensor we showed that a mastoparan prepore exists (see Section 3.4). The ratio of degree of v_4 activation in $IMKP_{0.3-6}$ and $IMLiP_{0.3-6}$ of this peptide is less than the ratio of the transference number of K^+ and Li^+. Such ratio of degree of v_4 activation of melitin is less than that of TAM. This agrees with literature data on model membranes. In liposomes TAM forms channels characterized by much (20- to 100-fold) longer lifetimes (Stankowski et al., 1991) compared with melittin (Matsuzaki et al., 1997). Using this biosensor a peptide is added to the inner mitochondrial membrane at the side of positive potential, and this is crucial for the effect of melittin (Pawlak et al., 1991). We do realize that RLM considered in this study as a biosensor are functionally active in a relatively narrow range of pH, temperature, and osmotic pressure. The number of “harmless” cations suitable for calibration of the RLM channels is rather limited (K^+, Li^+, $Tris^+$), but sufficient for evaluation of pore diameter corresponding to the lowest-conductance sub-state of alamethicin (Figs. 7 and 8). At the same time, RLM as the biosensor have some additional advantages. Cation entry into liposomes increases osmotic pressure and membrane tension which also influences alamethicin pores (Opsahl and Webbt, 1994). Mitochondrial swelling (in response to cation entry into the mitochondrial matrix) only stretches mitochondrial cristae, and the inner mitochondrial membrane remains unbroken for a rather long time (see Section 3.1, Fig. 1). In contrast to liposomes, mitochondria are rather large objects, and differences in sizes of individual organelle in a preparation of heavy RLM can be ignored. In the model system (BLM) this could be achieved by means of the “single-channel method”, which excludes the investigation of dependences of pore formation on peptide concentration.

A direct approach for investigation of the relationship between degree of alamethicin channel oligomerization and conductivity by using dimers and tetramers cross-liked by means of a flexible linker (attempts to stabilize the lowest-conductance sub-states of this peptide in BLM) did not give clear results (Huang, 2006). This shows the need for using indirect approaches. We propose a hypothesis explaining why mitochondria perform time-dependent discrimination of PTC induced by fractions of lowly and highly oligomeric alamethicin channels (see Fig. 7). The inner membrane of RLM is preferentially “filled” with hydrophobic proteins. Proteins and monomers of pore formers participating in two-dimensional diffusion are “coated” by a lipid shell. This makes their collisions “non-elastic”, and contacts formed during collisions have rather long lifetime. At reasonably low concentration of alamethicin in the membrane (C_m = 40 μM, peptide/lipid ratio of 1/6250) formal

free run between collisions of alamethicin monomers may be significantly higher than in BLM or liposomes (at the same peptide/lipid ratio). Thus, the biosensor provides evident advantages compared with traditional methods.

The understanding of mechanism of peptides pore formation may be useful for evaluation of their toxic effects on mitochondria. The therapeutic effect of pore formers is accompanied by decrease of mitochondrial $\Delta\Psi$. However, the magnitude of activation of v_4 by different pore formers does not correlate with the effect on this $\Delta\Psi$. The understanding of mechanism of peptides pore formation may be useful for evaluation of such toxic effect. We have shown that peptides that form pre-pore (mastoparan and melittin) have not radically dissipated mitochondrial $\Delta\Psi$. In the presence of mastoparan and melittin (compared with alamethicin and TAM) mitochondria retain stable $\Delta\Psi$, so these peptides may be potentially less harmful. The comparison of A_{200} and CLC/A_{200} of the series of modifications of individual natural peptides may be used for comparative testing of perspective pharmaceuticals on their hepatotoxicity.

Conflict of interest statement

None of the authors have any conflict of interest to disclose.

References

Aliverdieva, D.A., Sholtz, K.F., 1984. Quantitative determination of total mitochondrial protein with Coomassie. Prikl. Biokhim. Mikrobiol. 20, 823–830.

Aliverdieva, D.A., Mamaev, D.V., Lagutina, L.S., 2009. Parameters of the succinate transport into *Saccharomyces cerevisiae* cells after prolonged cold preincubation. Appl. Biochem. Microbiol. 45, 517–524.

Belosludtsev, K., Saris, N.E., Andersson, L.C., Belosludtseva, N., Agafonov, A., Sharma, A., Moshkov, D.A., Mironova, G.D., 2006. On the mechanism of palmitic acid-induced apoptosis: the role of a pore induced by palmitic acid and Ca^{2+} in mitochondria. J. Bioenerg. Biomembr. 38, 113–120.

Bondarenko, D.I., Mamaev, D.V., Sholts, K.F., 1996. Localization of substrate binding sites in the mitochondrial dicarboxylate transporter. Dokl. Acad. Nauk. 349, 408–410.

Brierley, G.P., Baysal, K., Jung, D.W., 1994. Cation transport systems in mitochondria: Na^+ and K^+ uniports and exchangers. J. Bioenerg. Biomembr. 26, 519–526.

Cabrera, M.P.S., Costa, S.T.B., de Souza, B.M., Palma, M.S., Ruggiero, J.R., Neto, J.R., 2008. Selectivity in the mechanism of action of antimicrobial mastoparan peptide Polybia-MP1. Eur. Biophys. J. 37, 879–891.

Duclohier, H., 2010. Antimicrobial peptides and peptaibols, substitutes for conventional antibiotics. Curr. Pharm. Des. 16, 3212–3223.

Emaus, R.K., Grunwald, R., Lemasters, J.J., 1986. Rhodamine 123 as a probe of transmembrane potential in isolated rat-liver mitochondria: spectral and metabolic properties. Biochim. Biophys. Acta 850, 436–448.

Fang-Yu, Chen, Ming-Tao, Lee, Huang Huey, W., 2002. Sigmoidal concentration dependence of antimicrobial peptide activities: a case study on alamethicin. Biophys. J. 82, 908–914.

Fehri, L.F., Wroblewski, H., Blanchard, A., 2007. Activities of antimicrobial peptides and synergy with enrofloxacin against *Mycoplasma pulmonis*. Antimicrob. Agents chemother. 51, 468–474.

Gauldie, J., Hanson, J.M., Rumjanek, F.D., Shipolini, R.A., Vernon, C.A., 1976. The peptide components of bee venom. Eur. J. Biochem. 61, 369–376.

Gaussin, V., Gailly, P., Gillis, J.M., Hue, L., 1997. Fructose-induced increase in intracellular free Mg^{2+} ion concentration in rat hepatocytes: relation with the enzymes of glycogen metabolism. Biochem. J. 326, 823–827.

Gracheva, O.A., Sokolova, A.E., Privalov, P.L., Lev, A.A., 1979. Development of salt-dependent and cation-specific states of lipid bilayer in the presence of valinomycin. Dokl. Akad. Nauk SSSR 246, 986–990.

Habermann, E., Kowallek, H., 1970. Modifications of amino groups and tryptophan in melittin as an aid to recognition of structure-activity relationships. Hoppe-Seyler's Z. Physiol. Chem. 351, 884–890.

Hanke, W., Boheim, G., 1980. The lowest conductance state of the alamethicin pore. Biochim. Biophys. Acta 596, 456–462.

Helluin, O., Dugast, J.-Y., Molle, G., Mackie, A.R., Ladha, S., Duclohier, H., 1997. Lateral diffusion and conductance properties of a fluorescein-labelled alamethicin in planar lipid bilayers. Biochim. Biophys. Acta 1330, 284–292.

Hendler, R.W., Shrager, R.I., 1987. Problems in the experimental determination of substrate-specific H^+/O ratios during respiration. J. Bioenerg. Biomembr. 19, 551–569.

Huang, H.W., 2006. Molecular mechanism of antimicrobial peptides: the origin of cooperativity. Biochim. Biophys. Acta 1758, 1292–1302.

Hunt, G.R., Jones, I.C., 1982. Lanthanide-ion transport across phospholipid vesicular membranes: a comparison of alamethicin 30 and A23187 using 1H-NMR spectroscopy. Biosci. Rep. 11, 921–928.

Jang, E.J., Kim, S.H., Yang, S.C., Lee, S.M., Choi, S.M., 2011. Melittin restores proteasome function in an animal model of ALS. J. Neuroinflammation 2011 (8), 69.

Kamath, V., Kyathanahalli, C.N., Jayaram, B., Syed, I., Olson, L.K., Ludwig, K., Klumpp, S., Krieglstein, J., Kowluru, A., 2010. Regulation of glucose- and mitochondrial fuel-induced insulin secretion by a cytosolic protein histidine phosphatase in pancreatic beta-cells. Am. J. Physiol. Endocrinol. Metab. 299, E276–286.

Kempf, C., Klausner, R.D., Weinstein, J.N., Renswoude, J.V., Pincus, M., Blumenthal, R., 1982. Voltage-dependent trans-bilayer orientation of melittin. J. Biol. Chem. 257, 2469–2476.

Kessel, A., Tieleman, D.P., Ben-Tal, N., 2004. Implicit solvent model estimates the stability of model structures of the alamethicin channel. Eur. Biophys. J. 33, 16–28.

Kim, S.J., Park, J.H., Kim, K.H., Lee, W.R., Kim, K.S., Park, K.K., 2011. Melittin inhibits atherosclerosis in LPS/high-fat treated mice through atheroprotective actions. J. Atheroscler. Thromb. 18, 1117–11126.

Laatikainen, M., Sainio, T., Davankov, V., Tsyurupa, M., Blinnikova, Z., Paatero, E., 2007. Modeling of size-exclusion chromatography of electrolytes on non-ionic nanoporous adsorbents. J. Chromatogr. 1149, 245–253.

Lee, M.T., Hung, W.C., Chen, F.Y., Huang, H.W., 2008. Mechanism and kinetics of pore formation in membranes by water-soluble amphipathic peptides. Proc. Natl. Acad. Sci. USA 105, 5087–5092.

Lee, W.R., Park, J.H., Kim, K.H., Park, Y.Y., Han, S.M., Park, K.K., 2011. Protective effects of melittin on transforming growth factor-β1 injury to hepatocytes via antiapoptotic mechanism. Toxicol. Appl. Pharmacol. 256, 209–215.

Lenton, L.M., Behm, C.A., Bygrave, F.L., 1995. Aberrant mitochondrial respiration in the livers of rats infected with *Fasciola hepatica*: the role of elevated non-esterified fatty acids and altered phospholipid composition. Biochem. J. 307, 425–431.

Matsuzaki, K., Yoneyama, S., Murase, 0., Miyajima, K., 1996. Transbilayer transport of ions and lipids coupled with mastoparan X translocation. Biochemistry 35, 8450–8456.

Matsuzaki, K., Yoneyama, S., Miyajima, K., 1997. Pore formation and translocation of melittin. Biophys. J. 73, 831–838.

Mereuta, L., Asandei, A., Luchian, T., 2011. Meet me on the other side: trans-bilayer modulation of a model voltage-gated ion channel activity by membrane electrostatics asymmetry. PLoS One 6, e25276.

Miroshnikov, A.I., Snezkova, L.G., Nazimov, I.V., Reshetova, O.I., Rozykov, B.V., Gushin, I.S., 1981. Structure and properties of histamine-releasing peptides from *Vespa orientalis* venom. Bioorg. Chem. 7, 1467–1478.

Mosolova, I.A., Gorskaya, I.A., Sholtz, K.F., Kotelnikova, A.V., 1971. Preparation from rat liver of tightly coupled mitochondria with storage stability. Vopr. Med. Khim. 17, 286–290.

Mottamal, M., Lazaridis, T., 2006. Voltage-dependent energetics of alamethicin monomers in the membrane. Biophys. Chem. 122, 50–57.

Naumowicz, M., Kotynska, J., Petelska, A., Figaszewski, Z., 2006. Independence analysis of phosphatiylcholine membranes modified with valinomycin. Eur. Biophys. J. 35, 238–246.

Opsahl, L.R., Webbt, W.W., 1994. Transition of membrane tension by the ion channel alamethicin. Biophys. J. 66, 71–74.

O'Rourke, B., 2007. Mitochondrial ion channels. Annu. Rev. Physiol. 69, 19–49.

Park, J.H., Kum, Y.S., Lee, T.I., Kim, S.J., Lee, W.R., Kim, B.I., Kim, H.S., Kim, K.H., Park, K.K., 2011. Melittin attenuates liver injury in thioacetamide-treated mice through modulating inflammation and fibrogenesis. Exp. Biol. Med. 2011 (236), 1306–1313.

Park, J.H., Kim, K.H., Lee, W.R., Han, S.M., Park, K.K., 2012. Protective effect of melittin on inflammation and apoptosis in acute liver failure. Apoptosis 17, 61–69.

Pawlak, M., Stankowski, S., Schwarz, G., 1991. Melittin induced voltage dependent conductance in DOPC lipid bilayers. Biochim. Biophys. Acta 1062, 94–102.

Pfeiffer, D.R., Gudz, T.I., Novgorodov, S.A., Erdahl, W.L., 1995. The peptide mastoparan is a potent facilitator of the mitochondrial permeability transition. J. Biol. Chem. 270, 4923–4932.

Polozov, I.V., Polozova, A.I., Tytler, E.M., Anantharamaiah, G.M., Segrest, J.P., Woolley, G.A., Epand, R.M., 1997. Role of lipids in the permeabilization of membranes by class L amphipathic helical peptides. Biochemistry 36, 9237–9245.

Raghuraman, H., Chattopadhyay, A., 2007. Melittin: a membrane-active peptide with diverse functions. Biosci. Rep. 27, 189–223.

Ravdel, A.A., Ponomareva, A.M. (Eds.), 2003. A Short Reference Book of Physicochemical Parameters, Ivan Fedorov, SPb.

Rinehart Jr., K.L., Cook Jr., J.C., Meng, H., Olson, K.L., Pandey, R.C., 1977. Mass spectrometric determination of molecular formulas for membrane-modifying antibiotics. Nature 269, 832-823.

Romani, A., 2007. Regulation of magnesium homeostasis and transport in mammalian cells. Arch. Biochem. Biophys. 458, 90–102.

Saint-Macary, M., Foucher, B., 1985. Comparative partial purification of the active dicarboxylate transport system of rat, kidney and heart mitochondria. Biochem. Biophys. Res. Commun. 113, 498–504.

Schwarz, G., Reiter, R., 2001. Negative cooperativity and aggregation in biphasic binding of mastoparan X peptide to membranes with acidic lipids. Biophys. Chem. 90, 269–277.

Sengupta, D., Leontiadou, H., Mark, A.E., Marrink, S.J., 2008. Toroidal pores formed by antimicrobial peptides show significant disorder. Biochim. Biophys. Acta 1778, 2308–2317.

Shipolini, R.A., Callewaert, G.L., Cottrell, R.C., Doonan, S., Vernon, C.A., Banks, B.E., 1971. Phospholipase A from bee venom. Eur. J. Biochem. 20, 459–468.

Sholtz, K.F., Zakharova, T.S., 1980. In: Kretovich, V.L., Sholtz, K.F. (Eds.), Biochemical Methods. Nauka, Moscow.

Sholtz, K.F., Reznik, G.I., Solov'eva, N.A., Shezhkova, L.G., Miroshnikov, A.I., 1980a. Effects of melittin and its tetraacetyl derivative on rat liver mitochondria. Biokhimiia 45, 1840–1849.

Sholtz, K.F., Aliverdieva, D.A., Snezhkova, L.G., Miroshnikov, A.I., Kotel'nikova, A.V., 1983. Action of the mastoparan from hornet venom on mitochondria. Dokl. Akad. Nauk SSSR 273, 747–750.

Sholtz, K.F., Aliverdieva, D.A., Kotel'nikova, A.V., 1985. Action of alamethicin on the coupling membrane of mitochondria. Dokl. Akad. Nauk SSSR 283, 723–727.

Sholtz, K.F., Mamaev, D.V., Bondarenko, D.I., Lagutina, L.S., 1990. Characteristics of the interaction between 2-alkylmalonates and the substrate-binding site of the dicarboxylate carrier of rat liver mitochondria. Biokhimiia 55, 1832–1840.

Shpakov, A.O., 2009. Polycationic peptides as nonhormonal regulators of chemosignal systems. Z. Evol. Biokhim. Phyziol. 45, 355–367.

Qian, Shuo., Wang, Wangchen., Yang, Lin., Huang, Huey.W., 2008. Structure of the alamethicin pore reconstructed by X-ray diffraction analysis. Biophys. J. 94, 3512–3522.

Stankowski, S., Pawlak, M., Kaisheva, E., Robert, C.H., Shwarz, G., 1991. A combined study of aggregation, membrane affinity and pore activity of natural and modified milittin. Biopchim. Biophys. Acta 1069, 77–86.

Szewczyk, A., Jarmuszkiewicz, W., Kunz, W.S., 2009. Mitochondrial potassium channels. IUBMB Life 61, 134–143.

Takei, J., Remenyi, A., Dempsey, C.E., 1999. Generalised bilayer perturbation from peptide helix dimerisation at membrane surfaces: vesicle lysis induced by disulphide-dimerised melittin analogues. FEBS Lett. 442, 11–14.

Wolkow, C.A., Iser, W.B., 2006. Uncoupling protein homologs may provide a link between mitochondria, metabolism and lifespan. Ageing Res. Rev. 5, 196–208.

Yu, K., Kang, S., Kim, S.D., Ryu, P.D., Kim, Y., 2001. Interactions between mastoparan B and the membrane studied by 1H NMR spectroscopy. J. Biomol. Struct. Dyn. 18, 595–606.

Zoratti, M., Szabo, I., 1994. Electrophysiology of the inner mitochondrial membrane. J. Bioenerg. Biomembr. 26, 543–553.